# Lattice dynamics of the fullerenes $M_xC_{60}$

K. N. Prabhatasree and S. L. Chaplot
*Solid State Physics Division, Bhabha Atomic Research Centre, Trombay, Mumbai 400 085, India*
(Received 9 August 2000; published 1 February 2001)

Lattice dynamical calculations of the phonon density of states of external modes are reported for $K_3C_{60}$, $Rb_3C_{60}$, and $Rb_6C_{60}$ using three different models of transferable interatomic potentials. On comparison with the experimental reported data, an interatomic potential consisting of Coulomb and short range interactions has been found most suitable to explain the phonon density of states of the systems studied. Calculations using the rigid molecular ion model have enabled assignment of various important features in the experimental phonon spectra in terms of the vibrations of different species.

DOI: 10.1103/PhysRevB.63.085407 PACS number(s): 61.48.+c, 63.20.Dj, 74.70.Wz

## I. INTRODUCTION

Since Krastchmer *et al.*[1(a)] produced macroscopic quantities of fullerene, knowledge of the molecular and solid state chemistry of $C_{60}$ has had rapid growth. Solid $C_{60}$ is a van der Waals bonded molecular crystal having a close packed face-centered cubic structure at 300 K.[2(a)] Alkali metals can be doped into the $C_{60}$ lattice to form $M_xC_{60}$ compounds, where $x=1-6$. Reports of superconductivity at 19 K and 29 K in potassium and rubidium doped $C_{60}$ motivated intense research toward understanding these materials.[1(b)] Four distinct crystalline phases have been identified, namely, fcc(I) for the parent phase with $x=0$, fcc(II) for $x=3$, a body centered tetragonal phase with $x=4$, and a body centered cubic phase with $x=6$.[2(b)] $M_1C_{60}$ forms polymer chains that show dramatic changes when compared to pure $C_{60}$.[2(c)]

Among the four distinct crystalline phases of the doped fullerenes, the metallic character is greatest at the composition $M_3C_{60}$.[3] The symmetry of $M_3C_{60}$ is $Fm\bar{3}m$ where the $C_{60}$ molecules are distributed between two equally populated orientations with little residual disorder of the $C_{60}$ lattice, as shown by the low value of the Debye-Waller factor of the carbon atoms.[2(b)] $C_{60}$ doped to saturation with $M$ atoms forming $M_6C_{60}$ is found to be nonsuperconducting. These are body centered systems with space group $Im\bar{3}$ with $C_{60}$ molecules orientationally ordered.[2(b),3]

It is of considerable interest to understand the kind of interatomic binding force existing in such samples, which in turn might help in understanding the occurrence of superconductivity in $M_3C_{60}$ systems. The inelastic neutron scattering technique is used to obtain information on the vibrational properties.[4] Phonon dispersion measurement on doped $C_{60}$ requires single crystals of these compounds, which has not yet been possible. Neutron scattering experiments on pristine polycrystalline samples have been carried out after attaining a high level of purity.

When alkali-metal atoms are intercalated into the $C_{60}$ lattice, they occupy the large interstices, i.e., the octahedral and tetrahedral voids in the lattice. The translational motions are stiffened a little; also the rotational hindrance potential is increased. As a result, librational frequencies are distinctly higher than in pure $C_{60}$. The intermolecular distances are also expanded slightly.[4,5(a)] In the case of $M_3C_{60}$, the $M$ atoms occupy all the available tetrahedral and octahedral vacancies of the host lattice. The local structure and dynamics of the alkali-metal atoms in $Rb_3C_{60}$, $K_2RbC_{60}$, etc., have been studied by extended x-ray-absorption fine-structure spectroscopy (EXAFS).[5(b)] In $M_6C_{60}$, the $M$ atoms are located at distorted tetrahedral sites such that each $C_{60}$ is surrounded by 24 $M$ atoms.[3]

In this paper, we report lattice dynamical calculations of the external vibrations for $Rb_3C_{60}$, $K_3C_{60}$, and $Rb_6C_{60}$ in the external mode approach.[6] In this approach, the well bound cluster of 60 carbon atoms, i.e., the $C_{60}$ molecule, is treated as a rigid body capable of both translation and rotation. Coupling is then allowed between the vibrations of this rigid body and those of other units and translations of the metal ions. The modes thus obtained are the external modes. The external modes extend up to about 15 meV while the internal modes of $C_{60}$ are seen above 30 meV.[5(a)] So they are well separated, and it is a reasonable approximation to ignore the coupling between the external and internal modes. Renker *et al.*[5(a)] previously reported lattice dynamical calculations in $K_3C_{60}$ and $Rb_3C_{60}$, using electrostatic and Lennard-Jones type potentials in the external mode approach. Different potential parameters were employed for the metal ions in different environments. We have now used lattice dynamical models based on transferable interaction potentials suitable for the three systems $Rb_3C_{60}$, $K_3C_{60}$, and $Rb_6C_{60}$, where identical potential parameters are employed for the same atomic pairs in the different systems. This potential may be further extended to explain the dynamics of systems like $Na_2RbC_{60}$.[5(c)]

Three different types of model have been used: a simple van der Waals (vdW) potential (model I); a van der Waals potential with an electrostatic interaction included (model II); and finally a screened Coulomb potential along with the van der Waals potential (model III). Comparison of the calculated results and the various structural and dynamical data indicates model II to be the most suitable. We have also calculated the partial phonon density of states due to the various constituents in the unit cell that contribute to the total density of states, which also helps in identifying the contributions from each one of the species to the various peaks in the observed phonon spectra. Our aim in doing these calculations has been to study the changes in the density of states due to intercalation, and to formulate an interatomic potential to explain these features.

 

## II. MODELS OF NONBONDED INTERATOMIC POTENTIALS

The various calculations to interpret the dynamics of doped fullerenes were done in the external mode approach.[6] This is justified since there is a large gap between the external and internal modes. The $C_{60}$ molecule was considered to be a single rigid unit, capable of both translation and rotation; hence the rigid molecular ion model was used. Coupling is allowed among the rigid fullerene molecules and the alkali-metal atoms. The force constants between the coupled vibrational degrees of freedom are calculated using models of interaction potentials. Here we are interested only in the interactions between nonbonded atoms, i.e., those between carbon atoms belonging to different $C_{60}$ molecules, between carbon and $M$ atoms, and between two $M$ atoms. Intramolecular interactions within $C_{60}$ contribute to its internal vibrations, which are not considered here.

### A. Model I

Initially a simple vdW type model was used. The form of the interatomic potential between any two atoms of species $i$ and $j$ separated by a distance $r$ in model I is

$$V_{ij}(r) = -A_{ij}/r^6 + B\exp[-Cr/(R_i+R_j)], \tag{1}$$

where $B=1822$ eV, and $C=12.364$;[7] $ij$ denotes the interaction between various species of atoms, i.e., C-C of two different $C_{60}$ rigid units, $M$-C, and $M$-$M$ interactions. $R_i$ denotes the radius associated with $M$ and carbon of the rigid $C_{60}$ unit. The values of $A_{\text{C-C}}$ for the carbon atom was taken as in previous studies on organic molecules and $C_{60}$.[7] The value of $A_{M\text{-}M}$ was assumed to be zero, i.e., no short range attractive interaction was assumed between the alkali-metal atoms.

### B. Model II

In the second model, electrostatic interactions were included in the interatomic potential. The form of the potential in model II is

$$V_{ij}(r) = -A_{ij}/r^6 + B\exp[-Cr/(R_i+R_j)] + Z_iZ_je^2/(4\pi\epsilon_0 r), \tag{2}$$

where $Z_i$ is the dimensionless number indicating the $i$ atom's fractional charge and $e$ is the electronic charge.

The Coulomb terms in the dynamical matrix for the various translational-translational, translational-rotational, and rotational-rotational coupling elements were rigorously calculated by the Ewald technique.[6]

### C. Model III

$M_3C_{60}$ are metallic systems, whereas pure $C_{60}$ and $Rb_6C_{60}$ are insulating in nature.[8] Owing to their metallic nature, a screened Coulombic potential was used for $M_3C_{60}$ systems as given by

TABLE I. Potential parameters used in the rigid molecular ion model calculations. $A_{\text{C-C}}=387.87$ kcal/mol; $R_{\text{K}}=2.2$ Å; $R_{\text{Rb}}=2.6$ Å; $R_{\text{C}}=1.75$ Å.

| | $K_3C_{60}$ | $Rb_3C_{60}$ | $Rb_6C_{60}$ |
|---|---|---|---|
| | $A_{M\text{-C}}$ (kcal/mol) | | |
| Model I | 2300 | 5050 | 5050 |
| Model II | 2000 | 4900 | 4900 |
| Model III | 2250 | 5050 | |
| | $Z_M$ | | |
| Model II | 0.5 | 0.5 | 0.75 |
| Model III | 1.0 | 1.0 | |
| | Experimental $a$ (Å) | | |
| | 14.24 | 14.42 | 11.54 |
| | Calculated $a$ (Å) | | |
| Model I | 14.26 | 14.45 | 11.80 |
| Model II | 14.29 | 14.42 | 11.55 |
| Model III | 14.26 | 14.43 | |

$$V_{ij}(r) = -A_{ij}/r^6 + B\exp[-Cr/(R_i+R_j)] + Z_iZ_j\exp(-k_0 r)e^2/(4\pi\epsilon_0 r), \tag{3}$$

where, $k_0$ is a screening parameter.[9] This screening parameter was calculated in the Thomas-Fermi formalism to be $k_0=1$ Å$^{-1}$ assuming three conduction electrons in the primitive cell of $M_3C_{60}$ for both potassium and rubidium systems.[9] However, we have carried out the calculation for a range of $k_0$ values from 0.1 to 1 Å$^{-1}$.

## III. CALCULATIONS

The calculations of the external modes of vibration for all the models were undertaken using the computer program DISPR.[10] The values of the potential parameters were determined so as to reproduce the experimental volume and the overall phonon spectra. As the structure of $M_3C_{60}$ involves two equally likely orientations of the $C_{60}$ molecules, we have chosen only one of the orientations for the lattice dynamical calculations. The potential parameters used for the various models are given in Table I.

The phonon density of states is defined as

$$g(\omega) = N\int_{BZ}\sum_j \delta[\omega-\omega_j(\mathbf{q})]d\mathbf{q}, \tag{4}$$

where $N$ is a normalization constant such that $\int g(\omega)d\omega = 1$; $\omega_j(\mathbf{q})$ is the phonon frequency of the $j$th normal mode of the phonon wave vector $\mathbf{q}$. Comparison with experimental data is done by computing the neutron weighted density of states given by

$$g^{(n)}(E) = A\sum_k \frac{4\pi b_k^2}{M_k} g_k(E), \tag{5}$$

where $A$ is the normalization constant, and $b_k$, $M_k$, and $g_k(E)$ are, respectively, the neutron scattering length, mass,

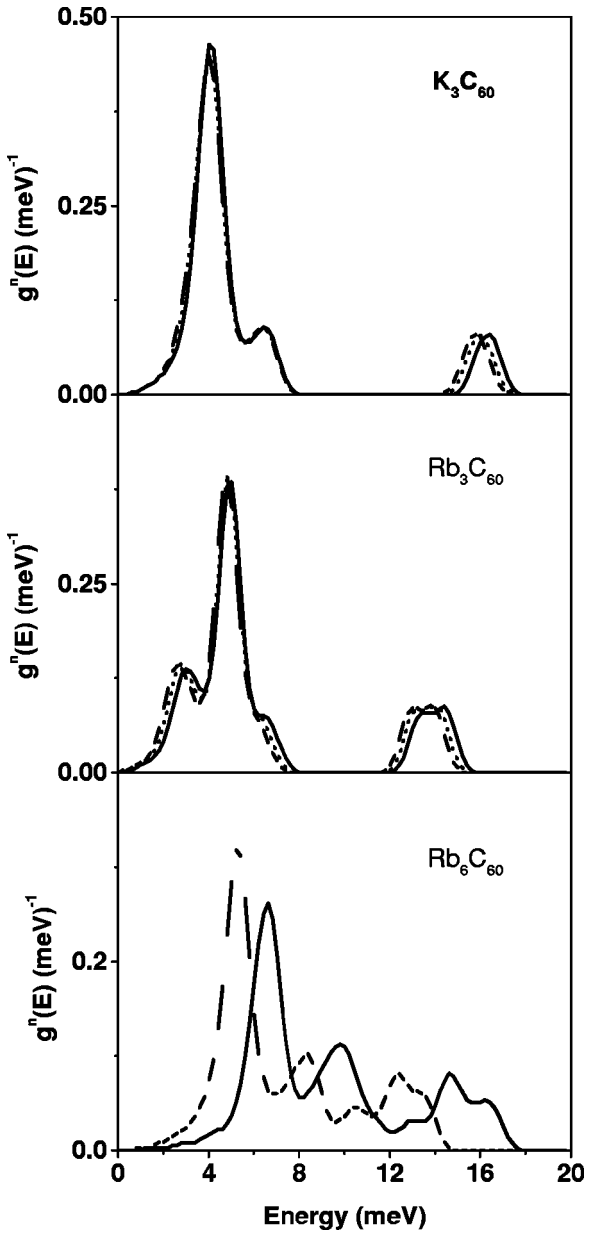


FIG. 1. Neutron weighted phonon density of states calculated using various models: model I, dashed line; model II, straight line; model III, dotted line ($k_0=0.22$ Å$^{-1}$). The spectra have been broadened with a Gaussian of full width at half maximum 1.0 meV.

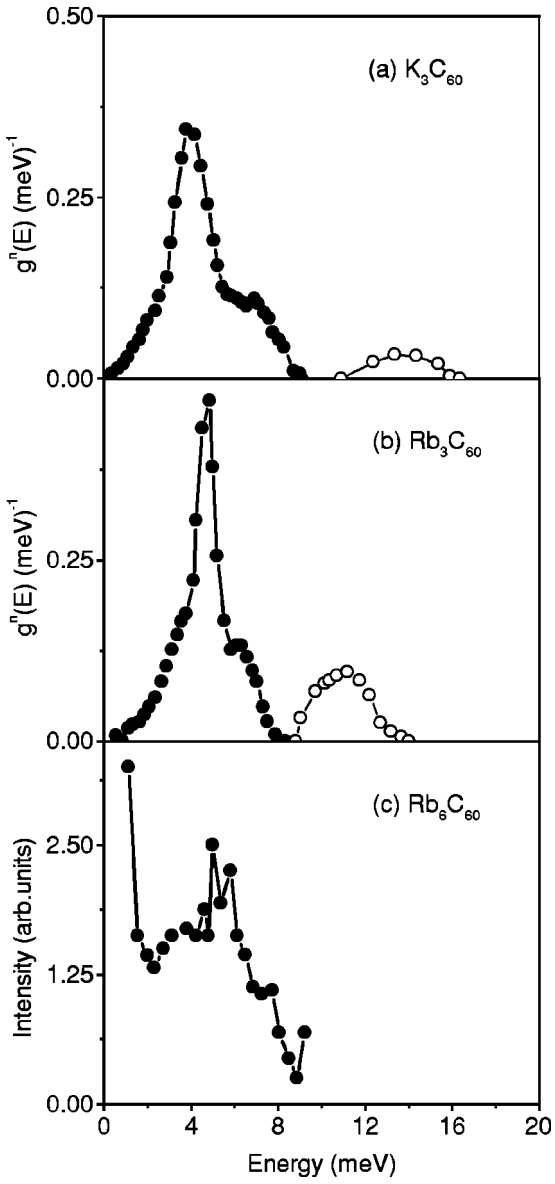


FIG. 2. The experimental phonon densities of states for (a) $K_3C_{60}$ (Ref. 5) and (b) $Rb_3C_{60}$ (Ref. 5). The open and full circles correspond to measurements with different resolutions. (c) The experimental neutron spectrum for $Rb_6C_{60}$ (Ref. 11).

and partial density of states of the constituent species. The values of $4\pi b_k^2/M_k$ for K, Rb, and C are 0.0434, 0.0743, and 0.4625 b/amu, respectively.

## IV. RESULTS AND DISCUSSION

The phonon densities of states obtained are given in Fig. 1 for $K_3C_{60}$, $Rb_3C_{60}$, and $Rb_6C_{60}$ using the three models discussed above. In the case of model III, the calculations shown were done using $k_0=0.22$ Å$^{-1}$. To start with, calculations were done from $k_0=0.1$ Å$^{-1}$ to $k_0=1$ Å$^{-1}$, which is the maximum possible value for screening for $K_3C_{60}$ and $Rb_3C_{60}$. Comparison of the data for the two extreme values of $k_0$ for both the systems showed very small differences, indicating negligible contribution from the screened Coulomb interaction. Since $M_6C_{60}$ is found to be insulating,[8] no screening is involved; therefore only models I and II have been used.

The experimental reported spectra are shown in Fig. 2.[5(a),11] Calculations using the different models enumerated above show good agreement with the reported results. The principal features of the density of states of $K_3C_{60}$, i.e., a shoulder around 3 meV, the peaks at 4 meV, and 7 meV, and a broad peak at 13.5 meV, and of $Rb_3C_{60}$, i.e., peaks at 3.5 meV, 4.8 meV, and 6.5 meV and a broad peak around 11 meV, are brought out well in all three models, although the contribution at the highest energy has been overestimated by about 2 meV in comparison with the experimental results.

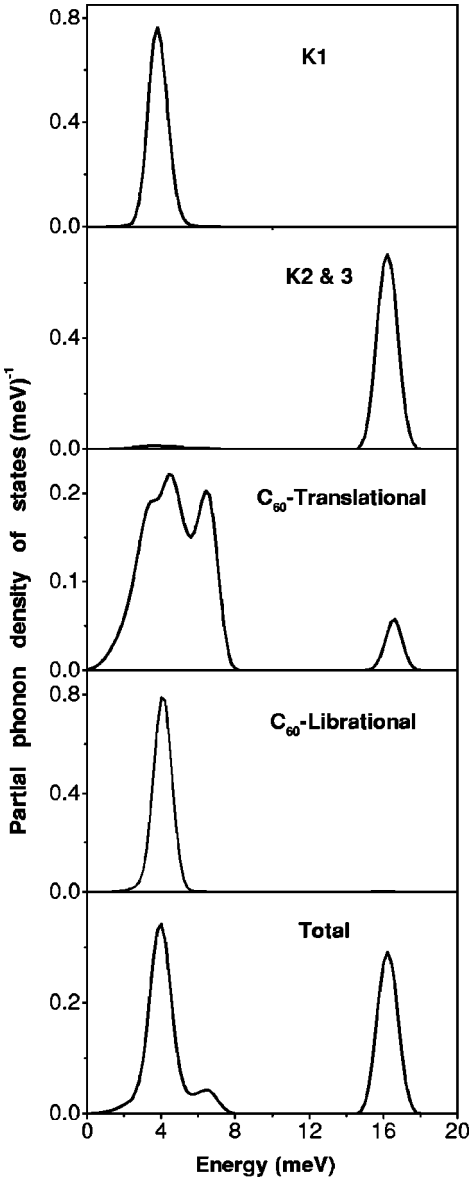


FIG. 3. Partial phonon density of states in $K_3C_{60}$ using model II. The potassium K1 at the octahedral site behaves differently from K2 and K3 at the tetrahedral site.

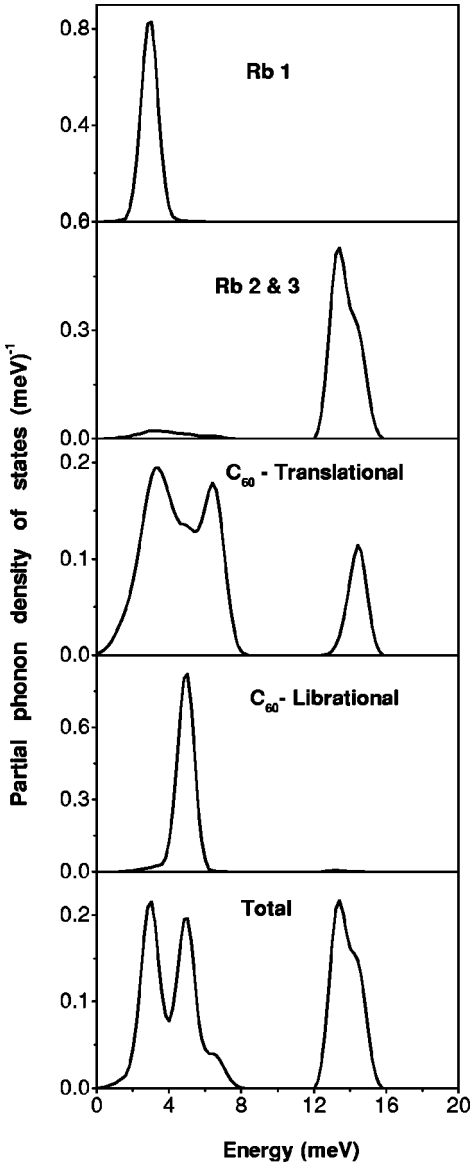


FIG. 4. Partial phonon density of states in $Rb_3C_{60}$ using model II. The rubidium Rb1 at the octahedral site behaves differently from Rb2 and Rb3 at the tetrahedral site.

We may note that the difference in the environments of the two metal ions leads to a large gap in the density of states in the case of $M_3C_{60}$, while no such gap occurs in $M_6C_{60}$ as all the metal ions are in identical environments.

All the models bring out a phonon density of states in good agreement with the reported experimental data. In the case of $K_3C_{60}$, the three curves due to the various models are almost superimposed except for the high energy band. In the case of $Rb_3C_{60}$ the three curves fall on top of each other within a very narrow band of 0.5 meV. In the case of $Rb_6C_{60}$ the structure of the density of states obtained is same for both models I and II, although the peaks shift toward higher energy in the spectra as we go from model I to model II. The main librational peak in model I is at a lower value of 5.2 meV, while the same peak occurs at 6.6 meV in model II, which is closer to the experimental peak value of 6 meV.[11,12] Hence it can be concluded that model II explains the density of states of all three systems satisfactorily.

The partial densities of each constituent of the three systems $K_3C_{60}$, $Rb_3C_{60}$, and $Rb_6C_{60}$ using model II, i.e., the model with the electrostatic interactions included, are shown in Figs. 3, 4, and 5, respectively. It can be seen that, of the three alkali-metal atoms in $M_3C_{60}$, in Figs. 3 and 4 the two at the tetrahedral sites behave differently from the one at the octahederal site. From EXAFS,[5(b)] the value of the local Debye temperature associated with the Rb atom at the tetrahedral site in $Rb_3C_{60}$ was obtained as $\theta_D = 165$ K. This value appears to be consistent with the corresponding calculated partial density of states in Fig. 4, which peaks at 14 meV. The partial densities of states are used to calculate the thermal amplitudes or the temperature factors of the various atoms. Table II gives a comparison between the calculated and experimental values of the temperature factors for alkali-

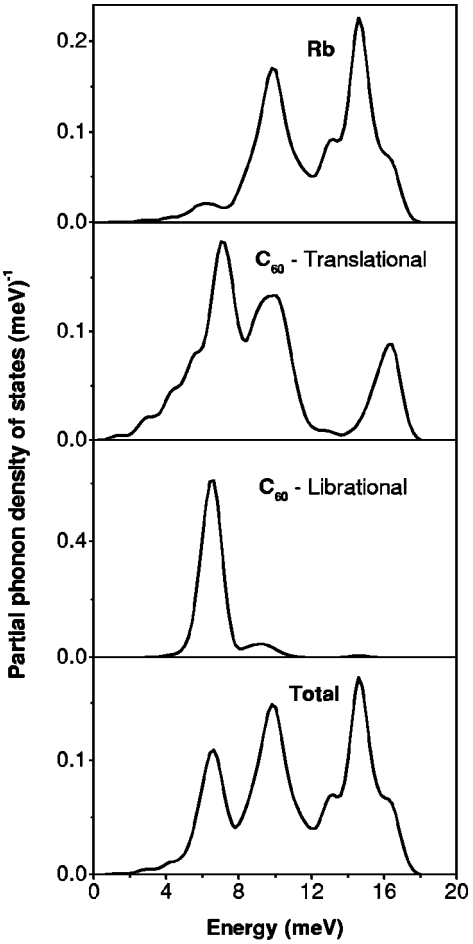


FIG. 5. Partial phonon density of states in $Rb_6C_{60}$ using model II. All the Rb here are in an identical distorted tetrahedral environment.

metal atoms and carbon in the $C_{60}$ molecule. In the case of the doped fcc systems, the alkali-metal atom at the octahedral interstitial void has greater space available to it, owing to which its thermal amplitude is greater and it gives a contribution in the lower energy range as against the other two alkali-metal atoms occupying the tetrahedral voids. The large thermal amplitude of the atoms at the octahedral site is consistent with the x-ray diffraction[13] and EXAFS experiments.[5(b)] An analysis of these experiments[5(b),13] as well as our calculations does not show evidence of any static site disorder at the octahedral sites, and therefore the observed thermal amplitudes are believed to arise only from lattice dynamics. From Figs. 3 and 4, it can be seen that the alkali-metal atom K1 at the octahedral site contributes at around 4 meV, while K2 and K3 at the tetrahedral sites contribute at around 16 meV in the case of $K_3C_{60}$; similarly, in the case of $Rb_3C_{60}$, Rb1 contributes at around 3 meV, while Rb2 and Rb3 contribute at around 14 meV. In the case of $Rb_6C_{60}$, all the Rb atoms are equivalent as expected[2(a),3] and contribute identically as given in Fig. 5.

TABLE II. Comparison of the isotropic temperature factors at 300 K, $B=(8\pi^2/3)[\langle u^2(x)\rangle+\langle u^2(y)\rangle+\langle u^2(z)\rangle]$(Å$^2$), for $K_3C_{60}$, $Rb_3C_{60}$, and $Rb_6C_{60}$ systems as derived from experiments (Ref. 13) and our calculations using model II. $M$=K,Rb.

| Experimental | | Calculated | |
|---|---|---|---|
| C | $M$ | C | $M$ |
| | $K_3C_{60}$ | | |
| 1.2±0.5 | 6.5±2 [a] | 1.6 | 1.6 [a] |
| | 16±6 [b] | | 15.6 [b] |
| | $Rb_3C_{60}$ | | |
| 1.0±0.3 | 2.0±0.5 [a] | 1.6 | 1.5 [a] |
| | 15±3 [b] | | 12.3 [b] |
| | $Rb_6C_{60}$ | | |
| 0.7±0.2 | 1.1±0.2 | 0.5 | 0.9 |

[a]Tetrahedral site.
[b]Octahdedral site.

The experimental data in Ref. 5(a) show that the libronic peak shifts toward higher energy as we go from pristine $C_{60}$ to metal doped $C_{60}$. As seen in Fig. 2, this shift further increases with increase in mass of the dopant and also with increased doping. The libronic peak in $K_3C_{60}$ is centered around 4 meV; in $Rb_3C_{60}$ it is centered around 5 meV. By this notion the libronic peak of $Rb_6C_{60}$ is expected above 6 meV. This reflects a stronger potential due to the ionic character of the fullerides. This observation holds good for the calculated results also. Libronic peaks of $K_3C_{60}$ and $Rb_3C_{60}$ occur around 4 meV and 5 meV, respectively, as seen in Figs. 3 and 4. The libronic peak of $Rb_6C_{60}$ is centered around 6.5 meV as seen in Fig. 5. We also note that both the experimental spectra and the calculations in $M_3C_{60}$ systems show that the contribution above 10 meV due to rubidium in $Rb_3C_{60}$ occurs at a lower energy as compared to that due to potassium in $K_3C_{60}$.

## V. CONCLUSIONS

In this paper, we have reported lattice dynamical calculations to explain the density of states in doped fullerene systems. We have used three different types of interatomic potential. From calculations with model III, it appears that screening does not play any vital role, since reducing the screening parameter $k_0$ to about one-tenth of its maximum value does not cause any perceivable change in the calculated density of states. Although model I, the simple van der Waal's interaction, gives a result in good agreement with experiment for metallic $M_3C_{60}$, the expected strong peak for $Rb_6C_{60}$ does not come out at the right energy using this model. Model II involving both the van der Waals and electrostatic interaction gives a good fit for all three systems. This model also substantiates the notion that the libronic contribution shifts to higher energy with increased doping as one goes from pure $C_{60}$ to alkali-metal doped systems.

[1] (a) W. Kratschmer, L.D. Lamb, K. Fostiropoulos, and D.R. Husmann, Nature (London) **347**, 354 (1990); (b) O. Gunnarsson, Rev. Mod. Phys. **69**, 575 (1997).

[2] (a) P.A. Heiney, J.E. Fischer, A.R. McGhie, W.J. Romanow, A.M. Denenstein, J.P. McCauley, Jr., A.B. Smith, and D.E. Cox, Phys. Rev. Lett. **66**, 2911 (1991); (b) O. Zhou and D.E. Cox, J. Phys. Chem. Solids **53**, 1373 (1992); (c) B. Renker, H. Schober, and R. Heid, Appl. Phys. A: Mater. Sci. Process. **64**, 271 (1997).

[3] O. Zhou, J.E. Fischer, N.C.S. Kycia, Q. Zhu, A.R. McGhie, W.J. Romanow, J.P. McCauley, Jr., A.B. Smith III, and D.E. Cox, Nature (London) **351**, 462 (1991).

[4] L. Pintschovius, Rep. Prog. Phys. **57**, 473 (1996).

[5] (a) B. Renker, F. Gompf, H. Schober, P. Adelmann, H.J. Bornemann, and R. Heid, Z. Phys. B: Condens. Matter **92**, 451 (1993); (b) G. Nowitzke, G. Wortmann, H. Werner, and R. Schlogl, Phys. Rev. B **54**, 13 230 (1996); (c) K. Prassides, C.M. Brown, S. Margadonna, K. Kordatos, K. Tanigaki, E. Suard, J. Dianoux, and K.D. Knudsen, J. Mater. Chem. **10**, 1443 (2000).

[6] G. Venkataraman and V.C. Sahni, Rev. Mod. Phys. **42**, 409 (1970).

[7] (a) S.L. Chaplot, A. Mierzejewski, G.S. Pawley, and J. Lefebvre, J. Phys.: Condens. Matter **2**, 2153 (1990); (b) L. Pintschovius and S.L. Chaplot, Z. Phys. B: Condens. Matter **98**, 527 (1995).

[8] P.W. Stephens, L. Mihaly, P.L. Lee, R.L. Whetten, S.M. Huang, R. Kaner, F. Diederich, and K. Holczer, Nature (London) **351**, 632 (1991).

[9] See N.W. Ashcroft and N.D. Mermin, *Solid State Physics* (CBS Publishing, Tokyo, 1987).

[10] S.L. Chaplot, BARC External Report No. 972, 1978 (unpublished).

[11] C. Christides, D.A. Neumann, K. Prassides, J.R.D. Copley, J.J. Rush, M.J. Rosseinsky, D.W. Murphy, and R.C. Haddon, Phys. Rev. B **46**, 12 088 (1992).

[12] H. Schober, B. Renker, F. Gompf, and P. Adelmann, Physica C **235-240**, 2487 (1994).

[13] P.W. Stephens and L. Mihaly, Phys. Rev. B **45**, 543 (1992).